

# Controlled Activation of Protein Rotational Dynamics Using Smart Hydrogel Tethering

Brenda M. Beech,<sup>†,‡</sup> Yijia Xiong,<sup>‡</sup> Curt B. Boschek,<sup>‡</sup> Cheryl L. Baird,<sup>‡</sup> Diana J. Bigelow,<sup>‡</sup> Kathleen McAteer,<sup>†</sup> and Thomas C. Squier<sup>\*,‡</sup>

<sup>†</sup>School of Biological Sciences, Washington State University Tri-Cities, Pullman, Washington 99164, United States

<sup>‡</sup>Biological Sciences Division, Fundamental Sciences Directorate, Pacific Northwest National Laboratory, Richland, Washington 99354, United States

**S** Supporting Information

**ABSTRACT:** Stimulus-responsive hydrogel materials that stabilize and control protein dynamics have the potential to enable a range of applications that take advantage of the inherent specificity and catalytic efficiencies of proteins. Here we describe the modular construction of a hydrogel using an engineered calmodulin (CaM) within a poly(ethylene glycol) (PEG) matrix that involves the reversible tethering of proteins through an engineered CaM-binding sequence. For these measurements, maltose binding protein (MBP) was isotopically labeled with <sup>13</sup>C and <sup>15</sup>N, permitting dynamic structural measurements using TROSY-HSQC NMR spectroscopy. The protein dynamics is suppressed upon initial formation of hydrogels, with a concomitant increase in protein stability. Relaxation of the hydrogel matrix following transient heating results in enhanced protein dynamics and resolution of substrate-induced large-amplitude domain rearrangements.

Proteins are widely used as sensors for analyte detection in a range of industrial processes taking advantage of the specificity and mild conditions associated with enzymatic reactions.<sup>1</sup> Further, the adaptable architecture of proteins facilitates their redesign to create high-affinity platforms capable of sensing and catalysis.<sup>2</sup> Practical applications typically require protein immobilization within material supports that stabilize proteins, enhance product purity, and facilitate protein reuse.<sup>1</sup> Methods used for protein immobilization involve nonspecific adsorption or cross-linking and are typically limited to proteins whose catalytic mechanisms do not involve large-amplitude domain motions. However, the functional immobilization of conformationally dynamic multidomain proteins, which typically involve shear or hinge motions, will require improved approaches [see the Supporting Information (SI) for protein examples].<sup>3</sup>

A promising approach might involve an existing protein-based hydrogel that harnesses large-amplitude protein motions.<sup>4</sup> For example, when a hydrogel composed of the calcium-binding protein calmodulin (CaM) bound within a poly(ethylene glycol) diacrylate (PEGDA) matrix is used, volume changes upon ligand binding to CaM permit the controlled release of entrapped peptides.<sup>5</sup> Building upon this architecture, we have developed a tethering approach to affinity immobilization of multidomain proteins within self-assembled hydrogels with mesh (pore) sizes

that are controlled by the dimensions (mass) of the PEGDA polymeric linker. Protein tethering involves engineering a sequence encoding the CaM-binding sequence from skeletal muscle myosin light-chain kinase (M13) onto the protein's C-terminus to facilitate self-assembly into functionalized hydrogels that contain CaM as part of a poly(ethylene glycol) (PEG) matrix (see the schematic illustration in the SI). High-affinity binding (i.e.,  $K_d < 1$  nM) is maintained between M13 and CaM following creation of an M13-fusion protein for tethering (see Figure S5 in the SI). Dynamic structural measurements of maltose binding protein (MBP) were used to identify the optimal material properties necessary for maintenance of function. MBP was chosen because of its well-understood rigid-body hinge-bending domain motions, where a 35° domain reorientation of the opposing domains upon substrate binding is necessary for formation of the complex with the ABC membrane protein transport complex.<sup>6</sup> Such large conformational changes in MBP are typical of multidomain proteins,<sup>7</sup> which do not commonly retain function following current immobilization methods and long-term storage.

Transverse-relaxation-optimized heteronuclear single-quantum correlation NMR spectroscopy (TROSY-HSQC)<sup>8</sup> was used to monitor the dynamics of <sup>13</sup>C/<sup>15</sup>N isotopically enriched MBP–M13 in solution and following hydrogel formation. For solution measurements, MBP–M13 was bound to an engineered CaM conjugated with a small PEG (575 Da) at two engineered cysteines (i.e., Cys<sub>34</sub> and Cys<sub>110</sub>) located on the opposing domains of CaM (i.e., CaM\*). The mass of MBP–M13 complexed to CaM\* is 66 kDa.<sup>9</sup> Data interpretation was facilitated by prior assignments of the correlation peaks for MBP in solution,<sup>10</sup> which demonstrated that substrate-dependent chemical shifts are principally restricted to interfacial regions between the opposing domains.<sup>10</sup>

TROSY-HSQC spectra of MBP–M13 bound to CaM\* (no hydrogel formation) show a large spectral dispersion (~3 ppm over <sup>1</sup>H and ~20 ppm over <sup>15</sup>N) with peak positions that are consistent with a well-folded protein complex with no evidence of aggregation (Figure 1). Similar spectral dispersion is apparent at all temperatures between 25 and 45 °C. In comparison to published <sup>15</sup>N-HSQC spectra of MBP (42 kDa), there are congruent peak distributions for MBP–M13 bound to

Received: July 3, 2014

Published: September 5, 2014

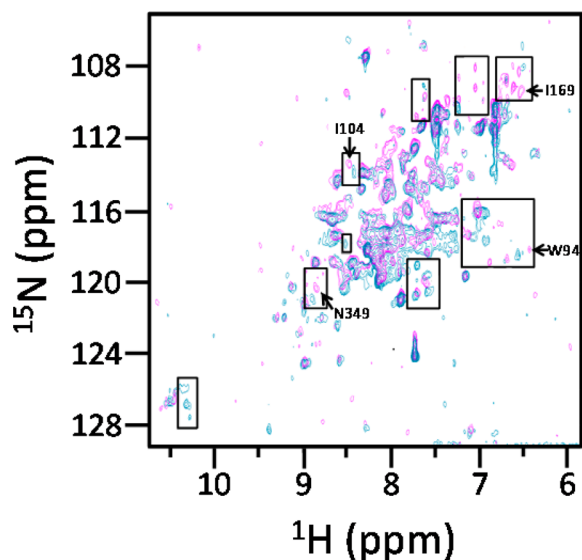


**Figure 1.** Resolution of maltose-induced structural changes in MBP. TROSY-HSQC NMR spectra of  $^{13}\text{C}$ ,  $^{15}\text{N}$ -labeled MBP-M13 (0.2 mM) bound to CaM\* in the absence (blue) and presence (pink) of maltose (20 mM). Spectra were obtained at 600 MHz in 50 mM HEPES (pH 7.5) and 10 mM  $\text{CaCl}_2$  at 25 °C (10% v/v  $\text{D}_2\text{O}$ ). Boxes (expanded in Figure S7) highlight diagnostic regions that undergo characteristic spectral shifts upon maltose binding.<sup>10,12</sup>

CaM\*.<sup>10,11</sup> The increased size of MBP-M13 bound to CaM\* (~66 kDa) results in reductions in spectral resolution and significantly broader resonances that preclude the quantitative assignment of individual peaks. Nevertheless, the positions of some well-resolved amino acids known to be highly sensitive to maltose-induced domain reorientations within MBP can be identified in the spectrum.<sup>10</sup> In all cases, there are characteristic chemical shifts associated with maltose binding that are consistent with those previously observed for MBP.<sup>12</sup> For example, large chemical shifts are observed for I104 and N349 upon maltose binding. Likewise, resonances previously shown to undergo large chemical shifts upon maltose binding to MBP in solution (i.e., F169 and W94) are well-resolved after maltose binding.<sup>10</sup> These measurements demonstrate ligand-induced structural changes for MBP-M13 bound to CaM\* (in the absence of hydrogel formation) and provide a baseline level of protein dynamics that can be used to guide the construction of hydrogel structures that maintain functional protein motions.

Amines on MBP-M13 were modified with a succinimidyl ester of Alexa Fluor 532 (Invitrogen, A10236), permitting a determination of the ability of hydrogels composed of PEG-conjugated CaM (PEG-CaM) to reversibly bind fluorescently labeled MBP-M13 (MBP-M13<sup>AF</sup>) (Figure 2). MBP-M13<sup>AF</sup> was mixed with PEG (10 kDa) diacrylate in the presence and absence of 10 mol % PEG-CaM\* prior to photoinitiated cross-linking and hydrogel formation (Figure S6). Following hydrogel formation, MBP-M13<sup>AF</sup> was retained within the hydrogel in a calcium-dependent manner. In the presence of the calcium chelator ethylene glycol tetraacetic acid (EGTA), the majority of MBP-M13<sup>AF</sup> diffuses out of the hydrogel at a rate very similar to that observed for hydrogels with no complexed CaM\* ( $t_{1/2} = 30 \pm 3$  min), yielding an apparent translational diffusion coefficient of  $20 \pm 10 \mu\text{m}^2/\text{s}$  (see the SI). The calcium-dependent binding of MBP-M13<sup>AF</sup> to CaM\* in hydrogels demonstrates that the polymerized CaM retains calcium-dependent structural changes and an ability to bind target peptides following complexation

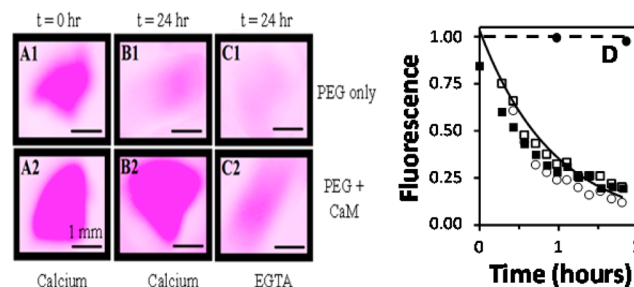


**Figure 2.** Calcium-dependent retention of bound MBP-M13 in hydrogel discs containing bound CaM. Fluorescent images (left panels) and time-dependent fluorescence intensity changes (right panel) of Alexa Fluor 532-labeled MBP-M13 (1  $\mu\text{M}$ ) in hydrogel discs (central material) composed of either polymerized PEG<sub>10K</sub> alone (10 mM) (top panels; squares) or upon inclusion of CaM\* (1.2 mM) (bottom panels; circles). The buffer was 50 mM HEPES (pH 7.5) in the presence of 10 mM  $\text{CaCl}_2$  (panels A and B; closed symbols) or 10 mM EGTA (panel C; open symbols). Images were taken (A) immediately following buffer exchange or (B, C) following incubation for 24 h.

within the hydrogel. Furthermore, the ability of MBP-M13<sup>AF</sup> to diffuse out of the hydrogel suggests that irrespective of the presence of CaM, the pore structure of the PEG matrix is adequate to permit facile diffusion and that sufficient mobility is present to permit large domain motions linked to substrate binding.

Upon polymerization of a preformed complex between MBP-M13 and CaM\* into hydrogels at 25 °C, there are large reductions in spectral resolution, with severe line broadening, in comparison with solution measurements (Figure 3A). Such line

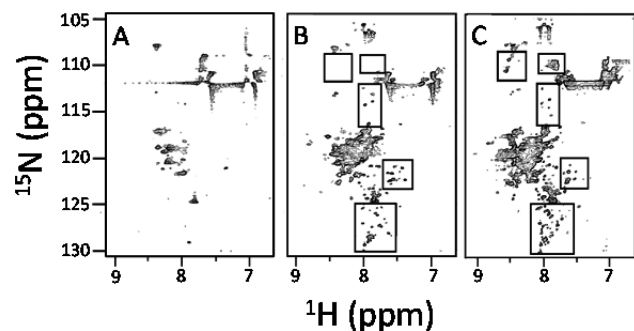


**Figure 3.** Temperature-dependent activation of protein dynamics in hydrogels. TROSY-HSQC NMR spectra of  $^{13}\text{C}$ ,  $^{15}\text{N}$ -labeled MBP-M13 bound to CaM\* in hydrogels (prepared essentially as described in the Figure 2 caption) at (A) 25 °C, (B) 40 °C, and (C) following a return to 25 °C in (A, B) the absence or (C) the presence of 20 mM maltose. Boxes (expanded in Figure S8) highlight resonances sensitive to conformational change upon maltose binding.

broadening is characteristic of a loss of motional averaging and commonly results from protein associations (e.g., associations between MBP-M13 and the hydrogel matrix).<sup>13</sup> Such interactions commonly enhance protein stability but may limit function through the disruption of important domain motions.<sup>7</sup>

Increasing the temperature to 40 °C results in significant increases in spectral resolution, with many well-resolved resonances at positions characteristic of a well-folded protein in solution (Figure 3B). No significant increase in spectral resolution is apparent at higher temperatures (all below the MBP unfolding temperature of 65 °C)<sup>14</sup> (Figure S1), indicating that the increases in spectral resolution arise as a result of increases in

motional averaging that are largely unrelated to global protein unfolding (although partially unfolded proteins may contribute, especially at 25 °C prior to transient heating). While less dramatic, similar increases in spectral resolution are apparent at 25 °C for MBP–M13 bound to CaM\* in hydrogels using higher-molecular-mass (i.e., longer) PEG linkers (Figure S2). Most significantly, the observed increases in protein mobility upon sample heating are retained following reduction of the sample temperature to 25 °C (Figure 3C), consistent with a model involving temperature-dependent alterations in the matrix structure that act to reduce molecular crowding between MBP–M13\* and the PEG matrix following transient heating. Upon addition of maltose, there are characteristic chemical shifts in resonances that are similar to those apparent for MBP–M13 in solution (see Figure 1). These results indicate that large-amplitude domain rearrangements associated with maltose binding are retained for MBP–M13 immobilized in these PEG hydrogels.

To better understand how transient heating alters the hydrogel matrix, we measured the translational diffusion of MBP–M13<sup>AF</sup> bound to CaM (not polymerized into the hydrogel matrix) within the hydrogel matrix using fluorescence photobleaching recovery (FPR). Following photobleaching, the rate of fluorescence recovery is directly related to the rate of translational diffusion (Figure 4). Upon transient heating

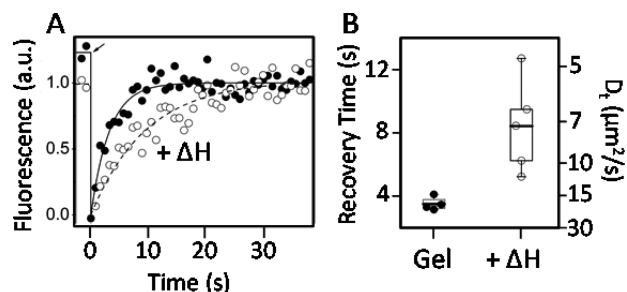


**Figure 4.** Stimulus-responsive hydrogel structural reorganization. (A) FPR curves and (B) translational diffusion coefficients ( $D_t$ ) calculated from measured recovery times for Alexa Fluor 555-labeled MBP–M13 bound to CaM\* freely diffusing in hydrogel sheets before (●) and after (○) transient heating ( $\Delta H = 37$  °C, 14 h).

(activation) there is an increase in the recovery time from 3.5 to 8 s, indicating a reduction in the rate of translational diffusion ( $D_t$ ) from about 20 to about  $8 \mu\text{m}^2/\text{s}$  (see the SI). The observed reductions in  $D_t$  upon transient heating are consistent with reductions in average pore size dimensions within the hydrogel, which are likely to arise from reductions in intermolecular contacts between tethered MBP in the hydrogel (Figure S6). Consistent with this interpretation, there are concomitant increases in protein mobility for the tethered MBP following hydrogel activation (Figure 3C).

To understand whether hydrogels modify protein stability, we compared the sensitivity of MBP–M13 bound to CaM\* in solution with that in hydrogels following addition of the protein denaturant guanidine hydrochloride (GdnHCl). Following incubation of MBP–M13 in solution with GdnHCl (1.0 M), there are reductions in spectral dispersion (Figure S3). Such peak broadening and spectral simplification is indicative of protein aggregation (which may arise following partial protein unfolding)<sup>15</sup> and is consistent with prior measurements indicating that MBP is destabilized and partially unfolded under these solution conditions.<sup>14,16</sup> The majority of peak

positions within the NMR spectrum are insensitive to the addition of maltose. Consistent with the interpretation that the majority of the protein has formed aggregates, there is increased light scattering and some protein precipitation (data not shown). In contrast, there are minimal alterations in the TROSY-HSQC spectrum for MBP–M13 bound to CaM\* within the hydrogel upon addition of 1 M GdnHCl (Figure S4). In these measurements, the small size of GdnHCl (mass = 95 Da) ensures facile access to the tethered MBP within the hydrogel. The decreased sensitivity of the protein fold to denaturation in the hydrogel indicates an increase in protein stabilization.

As already described, reductions in spectral resolution and associated peak broadening within the hydrogel (prior to heat activation) are indicative of macromolecular interactions between MBP–M13 and the hydrogel matrix. Such intermolecular interactions are consistent with our observations that MBP–M13 remains stable following drying and rehydration (permitting long-term storage under adverse conditions). Only upon heat activation is the hydrogel reconfigured to permit resolution of chemical shifts associated with maltose-induced domain reorientations. This is evident from the large increases in spectral resolution as well as the presence of substrate-induced chemical shifts that are similar to those observed for MBP–M13 in solution (Figure 3). The retention of substrate-induced domain movements for MBP–M13 in hydrogels following heat activation is consistent with prior measurements demonstrating the stabilization of many proteins in the presence of PEG and raffinose (or other nonreducing sugars).<sup>17</sup> These results demonstrate the utility of self-assembled hydrogels that undergo stimulus-responsive conformational changes to stabilize and control protein activation.

In conclusion, using a modular hydrogel construction that involves the self-assembly of preformed molecular complexes through an engineered peptide tether, we have identified a smart material suitable for protein immobilization and functional stabilization. Critical for the utility of hydrogel materials is the demonstration of enhanced protein stability. Our results further demonstrate an ability to take advantage of the conformational sensitivities of hydrogel materials to activate protein dynamics upon transient temperature increases. Such an approach permits storage of proteins in an immobilized state prior to their activation and will contribute to important applications that can take advantage of the specificity of proteins for a range of sensing and chemical transformation applications.<sup>18</sup> These smart materials possess optimized mass transfer properties (due to their high water content) (see Figure 4) and provide important avenues for ligand detection involving, for example, coassembly of multiple proteins that first bind and then catalytically act on bound ligands to amplify a signal associated with ligand binding.

## ■ ASSOCIATED CONTENT

### 📄 Supporting Information

MBP–M13 construct, procedures for protein labeling, formation of hydrogels, and ITC or TROSY-HSQC NMR data for MBP–M13 binding or effects of temperature, pore size, and denaturants on MBP mobility. This material is available free of charge via the Internet at <http://pubs.acs.org>.

## ■ AUTHOR INFORMATION

### Corresponding Author

tsquier@westernu.edu



**Notes**

The authors declare no competing financial interest.

**ACKNOWLEDGMENTS**

This work was supported by the Defense Threat Reduction Agency under HDTRA1-08-10-BRCWMD Award 10027-2828. Some measurements were performed at the Environmental Molecular Sciences Laboratory, a National Scientific User Facility supported by the Department of Energy's Office of Biological and Environmental Research and located at Pacific Northwest National Laboratory (PNNL).

**REFERENCES**

- (1) Sheldon, R. A.; van Pelt, S. *Chem. Soc. Rev.* **2013**, *42*, 6223.
- (2) (a) Mills, J. H.; Khare, S. D.; Bolduc, J. M.; Forouhar, F.; Mulligan, V. K.; Lew, S.; Seetharaman, J.; Tong, L.; Stoddard, B. L.; Baker, D. J. *Am. Chem. Soc.* **2013**, *135*, 13393. (b) Fry, H. C.; Lehmann, A.; Sinks, L. E.; Asselberghs, I.; Tronin, A.; Krishnan, V.; Blasie, J. K.; Clays, K.; DeGrado, W. F.; Saven, J. G.; Therien, M. J. *J. Am. Chem. Soc.* **2013**, *135*, 13914. (c) Giger, L.; Caner, S.; Obexer, R.; Kast, P.; Baker, D.; Ban, N.; Hilvert, D. *Nat. Chem. Biol.* **2013**, *9*, 494. (d) Tinberg, C. E.; Khare, S. D.; Dou, J.; Doyle, L.; Nelson, J. W.; Schena, A.; Jankowski, W.; Kalodimos, C. G.; Johnsson, K.; Stoddard, B. L.; Baker, D. *Nature* **2013**, *501*, 212. (e) Boschek, C. B.; Apiyo, D. O.; Soares, T. A.; Engelmann, H. E.; Pefaur, N. B.; Straatsma, T. P.; Baird, C. L. *Protein Eng., Des. Sel* **2009**, *22*, 325. (f) Hocker, B. *Biochem. Soc. Trans.* **2013**, *41*, 1137. (g) Sawyer, N.; Speltz, E. B.; Regan, L. *Biochem. Soc. Trans.* **2013**, *41*, 1131.
- (3) (a) Hudson, S.; Cooney, J.; Magner, E. *Angew. Chem., Int. Ed.* **2008**, *47*, 8582. (b) Gomes, D. E.; Lins, R. D.; Pascutti, P. G.; Lei, C.; Soares, T. A. *J. Phys. Chem. B* **2010**, *114*, 531.
- (4) (a) Peppas, N. A.; Huang, Y.; Torres-Lugo, M.; Ward, J. H.; Zhang, J. *Annu. Rev. Biomed. Eng.* **2000**, *2*, 9. (b) Kopecek, J.; Yang, J. *Polym. Int.* **2007**, *56*, 1078. (c) Ehrick, J. D.; Deo, S. K.; Browning, T. W.; Bachas, L. G.; Madou, M. J.; Daunert, S. *Nat. Mater.* **2005**, *4*, 298. (d) Banta, S.; Wheelton, I. R.; Blenner, M. *Annu. Rev. Biomed. Eng.* **2010**, *12*, 167.
- (5) (a) King, W. J.; Pytel, N. J.; Ng, K.; Murphy, W. L. *Macromol. Biosci.* **2010**, *10*, 580. (b) King, W. J.; Javeed, M.; Murphy, W. L. *Soft Matter* **2009**, *5*, 2399. (c) King, W. J.; Toepke, M. W.; Murphy, W. L. *Chem. Commun.* **2011**, *47*, 526. (d) King, W. J.; Toepke, M. W.; Murphy, W. L. *Acta Biomater.* **2011**, *7*, 975. (e) Murphy, W. L.; Dillmore, W. S.; Modica, J.; Mrksich, M. *Angew. Chem., Int. Ed.* **2007**, *46*, 3066.
- (6) (a) Sharff, A. J.; Rodseth, L. E.; Spurlino, J. C.; Quijoch, F. A. *Biochemistry* **1992**, *31*, 10657. (b) Quijoch, F. A.; Spurlino, J. C.; Rodseth, L. E. *Structure* **1997**, *5*, 997. (c) Tang, C.; Schwieters, C. D.; Clore, G. M. *Nature* **2007**, *449*, 1078.
- (7) Gerstein, M.; Krebs, W. *Nucleic Acids Res.* **1998**, *26*, 4280.
- (8) (a) Pervushin, K.; Riek, R.; Wider, G.; Wuthrich, K. *Proc. Natl. Acad. Sci. U.S.A.* **1997**, *94*, 12366. (b) Fernandez, C.; Wider, G. *Curr. Opin. Struct. Biol.* **2003**, *13*, 570.
- (9) (a) Boschek, C. B.; Squier, T. C.; Bigelow, D. J. *Biochemistry* **2007**, *46*, 4580. (b) Boschek, C. B.; Sun, H.; Bigelow, D. J.; Squier, T. C. *Biochemistry* **2008**, *47*, 1640. (c) Osborn, K. D.; Zaidi, A.; Mandal, A.; Urbauer, R. J.; Johnson, C. K. *Biophys. J.* **2004**, *87*, 1892.
- (10) Evenas, J.; Tugarinov, V.; Skrynnikov, N. R.; Goto, N. K.; Muhandiram, R.; Kay, L. E. *J. Mol. Biol.* **2001**, *309*, 961.
- (11) Gardner, K. H.; Zhang, X. C.; Gehring, K.; Kay, L. E. *J. Am. Chem. Soc.* **1998**, *120*, 11738.
- (12) Wright, C. M.; Majumdar, A.; Tolman, J. R.; Ostermeier, M. *Proteins* **2010**, *78*, 1423.
- (13) van Mierlo, C. P.; van den Oever, J. M.; Steensma, E. *Protein Sci.* **2000**, *9*, 145.
- (14) Ganesh, C.; Shah, A. N.; Swaminathan, C. P.; Surolia, A.; Varadarajan, R. *Biochemistry* **1997**, *36*, 5020.
- (15) Sugiki, T.; Yoshiura, C.; Kofuku, Y.; Ueda, T.; Shimada, I.; Takahashi, H. *Protein Sci.* **2009**, *18*, 1115.
- (16) Sheshadri, S.; Lingaraju, G. M.; Varadarajan, R. *Protein Sci.* **1999**, *8*, 1689.
- (17) (a) Dattelbaum, A. M.; Baker, G. A.; Fox, J. M.; Iyer, S.; Dattelbaum, J. D. *Bioconjugate Chem.* **2009**, *20*, 2381. (b) Minton, A. P.; Wilf, J. *Biochemistry* **1981**, *20*, 4821. (c) Jarvis, T. C.; Ring, D. M.; Daube, S. S.; von Hippel, P. H. *J. Biol. Chem.* **1990**, *265*, 15160. (d) Farrant, J. M.; Lehner, A.; Cooper, K.; Wiswedel, S. *Plant J.* **2009**, *57*, 65. (e) Poddar, N. K.; Ansari, Z. A.; Singh, R. K.; Moosavi-Movahedi, A. A.; Ahmad, F. *Biophys. Chem.* **2008**, *138*, 120.
- (18) Yan, L.; Zhu, Z.; Zou, Y.; Huang, Y.; Liu, D.; Jia, S.; Xu, D.; Wu, M.; Zhou, Y.; Zhou, S.; Yang, C. J. *J. Am. Chem. Soc.* **2013**, *135*, 3748.